

SOLUTION TO THE FERRORESONANT JUMP PROBLEM IN THREE-PHASE POWER CONDITIONING SYSTEMS

S.M. Miri, Member IEEE

Department of Electrical Engineering
The University of North Carolina
Charlotte, NC 28223

A. Keyhani, Member IEEE

Department of Electrical Engineering
The Ohio State University
Columbus, OH 43210

Abstract— A power conditioning system is a device used to improve the quality of power in order to reduce equipment malfunctions. In a three-phase power conditioning system which utilizes ferroresonant circuits, the improved quality results from the synthesis of output voltages which remain constant over a wide range of input voltage variations caused by voltage sags or surges, transients, noise, or harmonic distortions. This device is a highly nonlinear system with more than one possible steady state for a given input. Upon a change in inputs, the new steady state reached is determined by the parameter trajectories, and thus by the input trajectories, traced during the transient. In the literature, this problem has been referred to as the ferroresonant jump problem. Ferroresonant jump is a multimodal operation problem which occurs in both single and three-phase power conditioning systems. In the case of three-phase systems, this problem has never been studied and has no known solution. In this paper, an analytical investigation leading to a solution for the ferroresonant jump problem in three-phase conditioning systems is presented. The proposed solution has been successfully tested in the laboratory and can be easily implemented for the existing systems in the field.

Introduction

A problem known as ferroresonant jump associated with the operation of signal conditioning systems which use ferroresonant circuits has been reported in the literature [3,4,5,6,7,8]. Some researchers [6,7,8] have studied the occurrence of this phenomenon in single-phase conditioning systems with series or parallel ferroresonant circuits. In this paper, we study this problem in three-phase conditioning systems with parallel ferroresonant circuits. Fig. 1 shows the wiring diagram for the three-phase power conditioning system (PCS) [1]. The six interconnected saturating transformers TX1, TX2, TX3, TX4, TX5 and TX6 generate the building blocks for the synthesized output voltage waveforms. For a set of balanced input voltages V_{AB} , V_{BC} and V_{CA} , the exciting currents of the two-winding transformers TX4, TX5 and TX6 are a set of balanced currents. The exciting currents for the four-winding transformers TX1, TX2 and TX3 are

$$i_{E_1} = i_{E_4} - i_{E_6}$$

$$i_{E_2} = i_{E_5} - i_{E_4}$$

$$i_{E_3} = i_{E_6} - i_{E_5}$$

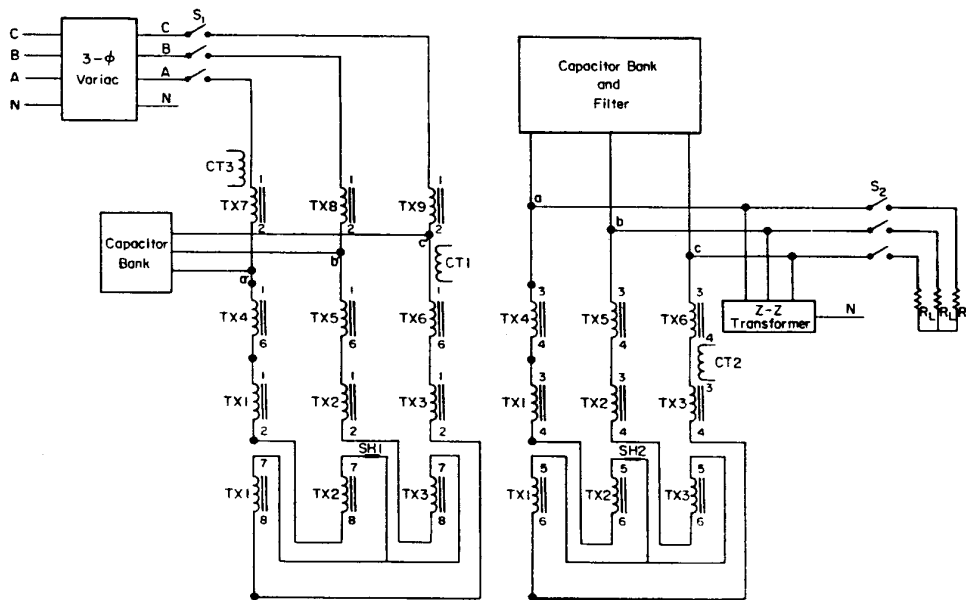


Fig. 1: Wiring diagram for the three-phase power conditioning system.

These six exciting currents can be shown on a phasor diagram (Fig. 2). The core of each transformer is designed to saturate at a specific level of its exciting current. A typical exciting current/flux relationship is depicted in Fig. 3. Also shown in this figure is a typical transformer winding voltage [2]. The levels of exciting currents at which transformer cores saturate, considering the phase shifts among the exciting currents, are set such that at any given time, five of the cores are in saturation and the sixth is in the linear region putting out a voltage pulse similar to that shown in Fig. 3. The unsaturating sequence can be determined from the phasor diagram of Fig. 2. This sequence is as follows: TX4 in positive direction (i.e., positive slope), TX1 in positive, TX6 in negative, TX3 in negative, TX5 in positive, TX2 in positive direction and so on. The magnitudes of the voltage pulses generated by the two-winding transformers are $\sqrt{3}$ times larger than those generated by the four-winding transformers. This results in a set of balanced sinusoidal line-to-line voltages at the output of the system.

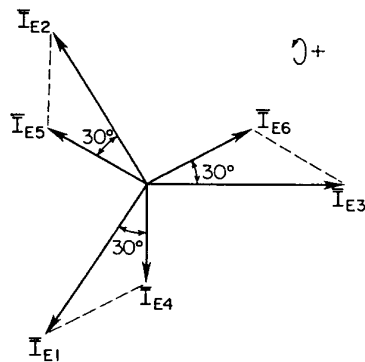


Fig. 2: PCS exciting currents.

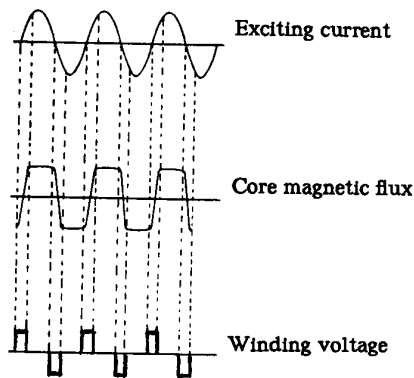


Fig. 3: A saturating transformer current, flux, and voltage relationships.

Due to nonlinearities of the six saturating transformers, this system has several modes of operation; one desirable (normal mode) and all others undesirable (oscillatory modes). An oscillatory mode of operation may be reached upon no-load start up or heavy load drops. In this mode, the saturating transformers do not saturate according to the intended sequence, and the desired parallel resonance between them and the capacitor banks does not occur. Instead, series resonance between the capacitor banks and the line chokes (TX7, TX8 and TX9) occurs, causing large currents to be drawn from the source.

The purpose of our study is to find ways of forcing the system into the desired steady state regardless of the transients occurring in the system. As a prerequisite, we have developed a model which closely mimics the behavior of the PCS shown in Fig. 1 during transient and steady state conditions [9]. The structure of this model is shown in Fig. 4.

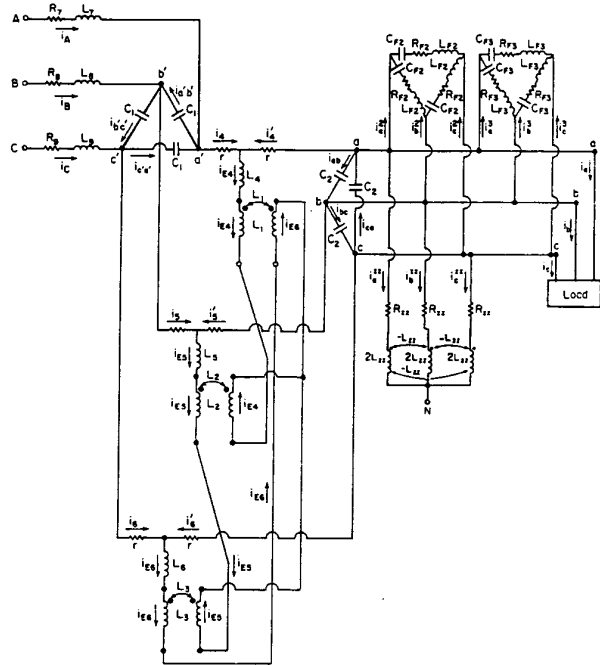


Fig. 4: Power conditioning system model structure.

Statement of the Problem

In the model of Fig. 4, the relations between flux linkages λ_j and exciting currents i_{E_j} in the six saturating transformers are modeled using Arctan functions. This results in estimates of incremental magnetizing inductances given by

$$\hat{L}_j(i_{E_j}) = \frac{\partial \hat{\lambda}_j}{\partial i_{E_j}} = \frac{a}{1 + bi_{E_j}^2}; \quad j = 1, 2, 3 \quad (1)$$

$$\hat{L}_j(i_{E_j}) = \frac{\partial \hat{\lambda}_j}{\partial i_{E_j}} = \frac{3a}{1 + 3bi_{E_j}^2}; \quad j = 4, 5, 6$$

with a and b some constants. It is due to nonlinearities of these inductances that the PCS exhibits different modes of operation (jump phenomenon). For a given set of balanced input voltages, there may be several stable waveforms for each exciting current of the six transformers, and thus, the system can reach any of the several possible steady states. The values of different system parameters (including the inductances) during the transient will determine the final steady state attained by the system. Our problem is to find ways, via design modifications, of forcing the system into the desired steady state regardless of the type of system transients which themselves depend on the uncontrollable factors such as changes in the system loads, system initial conditions, and the topology of the distribution system feeding the PCS.

Solution Procedure

The proposed solution to the ferroresonant jump problem begins with deriving an equation of the form $f(x) = 0$ where number of "acceptable" solutions for x would be equivalent to the number of possible steady states for a given set of balanced input voltages. The coefficients of this equation, which would be the parameters of the PCS, are then to be modified in a way that would result in only one "acceptable" solution for x . The first step in deriving such an equation is to develop a simplified circuit equivalent, in steady state, to the model of Fig. 4. Since the undesirable modes of operation occur under light to no-load conditions, the equivalent circuit is developed for the no-load condition. The details of developing such an equivalent circuit is given in [9]. This circuit (Fig. 5) has been developed under the assumptions of steady state operation, balanced 60 Hz input voltages, balanced 60 Hz line and exciting currents, and negligible winding and core resistances during steady state operation. In the equivalent circuit of Fig. 5, the voltage v represents the line-to-line voltage between any of the two phases, the voltage across the capacitor is the corresponding output voltage, i represents the corresponding line current, and i_E the corresponding exciting current. The inductances L_j are given by Eq. (1), and L' is used to denote the inductance of a line choke.

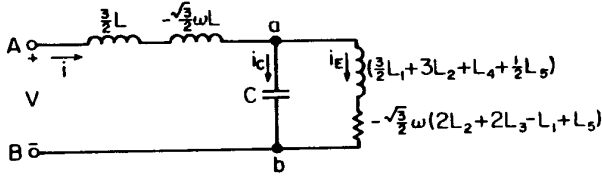


Fig. 5: Power conditioning system equivalent circuit for steady state analysis.

Referring to Fig. 5, our objective is now to derive an equation in terms of the line current i for a given input voltage v . For steady state operation, this equation is given by

$$\begin{aligned} v = & (R + R_{eq} - R_{eq}\omega^2 LC - L_{eq}\omega^2 RC)i \quad (2) \\ & + (L + R_{eq}RC + L_{eq} - L_{eq}\omega^2 LC)\frac{di}{dt} \\ & + (\omega^2 L_{eq}C)v - R_{eq}C\frac{dv}{dt} \end{aligned}$$

where

$$\begin{aligned} L & \triangleq \frac{3}{2}L' \\ R & \triangleq -\frac{\sqrt{3}}{2}\omega L' \\ L_{eq} & \triangleq \frac{3}{2}L_1 + 3L_2 + L_4 + \frac{1}{2}L_5 \\ R_{eq} & \triangleq -\frac{\sqrt{3}}{2}\omega(2L_2 + 2L_3 - L_1 + L_4) \end{aligned}$$

Under the assumption of balanced exciting currents, we can substitute for R_{eq} and L_{eq} in Eq. (2) by

$$\begin{aligned} R_{eq} & = -\frac{\sqrt{3}}{2}\omega \left[\frac{2a}{1+bi_{E2}^2} + \frac{2a}{1+bi_{E3}^2} - \frac{a}{1+bi_{E1}^2} + \frac{3a}{1+3bi_{E5}^2} \right] \\ L_{eq} & = \frac{3a}{2(1+bi_{E1}^2)} + \frac{3a}{1+bi_{E2}^2} + \frac{3a}{1+3bi_{E4}^2} + \frac{3a}{2(1+3bi_{E5}^2)} \end{aligned} \quad (3)$$

where for $i_E = i_{Ej}$, we have

$$\begin{aligned} i_{E1} & = \frac{3}{2}i_E - \frac{\sqrt{3}}{2\omega} \frac{di_E}{dt} \\ i_{E2} & = -\frac{3}{2}i_E - \frac{\sqrt{3}}{2\omega} \frac{di_E}{dt} \\ i_{E3} & = \frac{\sqrt{3}}{\omega} \frac{di_E}{dt} \\ i_{E5} & = -1/2(i_E + \frac{\sqrt{3}}{\omega} \frac{di_E}{dt}) \end{aligned} \quad (4)$$

For a given input voltage $v(t) = V_m \cos(\omega t + \theta)$, the fundamental solution of i_E (taken as reference) and that of i can be assumed to be of the forms

$$i_E(t) = I_E \cos \omega t \quad (5)$$

$$i(t) = I_m \cos(\omega t + \phi)$$

It has been shown in [9] that using Eqs. (3), (4), and (5), Eq. (2) can be written as the following two equations:

$$\begin{aligned} V_m \cos \theta & \left[\frac{1}{D}(3\omega^4 L^2 c^2 - \frac{3}{2}\omega^2 Lc)(J + \frac{3}{8}KbI_E^2) - \right. \\ & - \frac{3}{2D}\omega^2 Lc(\frac{3}{8}KbI_E^2 + \frac{1}{2}aP\omega^2 c) + (J + \frac{3}{8}KbI_E^2 - \frac{3}{2}aP\omega^2 c) + \\ & + \frac{3}{4D}a\omega^4 Lc^2(1 - \frac{3}{2}\omega^2 Lc)(P + QbI_E^2) + \frac{3}{2D}aP\omega^2 c(\frac{3}{2}LC - 1)^2 \left. \right] + \\ & + \sqrt{3}V_m \sin \theta \left[\frac{1}{2D}\omega^2 Lc(J + \frac{3}{8}KbI_E^2) + \frac{1}{D}(3\omega^4 L^2 c^2 - \frac{3}{2}\omega^2 Lc) \right. \\ & - (\frac{3}{8}KbI_E^2 + \frac{1}{2}aP\omega^2 c) + (\frac{3}{8}KbI_E^2 + \frac{1}{2}aP\omega^2 c) + \\ & + \frac{1}{2D}a\omega^2 c(1 - \frac{3}{2}\omega^2 Lc)^2(P + QbI_E^2) + \frac{3}{4D}aP\omega^4 Lc^2(\frac{3}{2}\omega^2 Lc - 1) \left. \right] - \\ & - \frac{\sqrt{3}}{D}I_E \left[\frac{1}{2}\omega L(J + \frac{3}{8}KbI_E^2) + 3\omega L(\omega^2 Lc - \frac{1}{2})(\frac{3}{8}KbI_E^2 + \frac{1}{2}P\omega^2 c) + \right. \\ & + \frac{1}{2}a\omega(1 - \frac{3}{2}\omega^2 Lc)^2(P + QbI_E^2) + \frac{3}{4}aP\omega^3 Lc(\frac{3}{2}\omega^2 Lc - 1) \left. \right] = 0 \end{aligned}$$

$$\begin{aligned}
& \sqrt{3}V_m \cos \theta \left[\frac{1}{2D}\omega^2 Lc(J - \frac{3}{8}KbI_E^2) + \frac{1}{D}(\frac{3}{2}\omega^2 Lc - 3\omega^4 L^2 c^2) \right. \\
& \left. (\frac{3}{8}KbI_E^2 + \frac{1}{2}aP\omega^2 c) - (\frac{3}{8}KbI_E^2 - \frac{1}{2}aP\omega^2 c) - \right. \\
& \left. - \frac{1}{2D}a\omega^2 c(1 - \frac{3}{2}\omega^2 Lc)^2(QbI_E^2 - P) - \frac{3}{4D}aP\omega^4 Lc^2 P(1 - \frac{3}{2}\omega^2 Lc) \right] \\
& + V_m \sin \theta \left[\frac{3}{2D}(\omega^2 Lc - 3\omega^4 L^2 c^2)(J - \frac{3}{8}KbI_E^2) - \right. \\
& \left. - \frac{3}{2D}\omega^2 Lc(\frac{3}{8}KbI_E^2 - \frac{1}{2}aP\omega^2 c) - (J - \frac{3}{8}KbI_E^2 - \frac{3}{2}aP\omega^2 c) + \right. \\
& \left. + \frac{3}{4D}a\omega^4 Lc^2(1 - \frac{3}{2}\omega^2 Lc)(QbI_E^2 - P) - \frac{3}{2D}a\omega^2 cP(1 - \frac{3}{2}\omega^2 Lc) \right] - \\
& - \frac{3}{D}I_E \left[\omega L(\frac{1}{2} - \omega^2 Lc)(J - \frac{3}{8}KbI_E^2) - \frac{1}{2}\omega L(\frac{3}{8}kbI_E^2 - \frac{1}{2}aP\omega^2 c) + \right. \\
& \left. + \frac{1}{4}a\omega^3 Lc(1 - \frac{3}{2}\omega^2 Lc)^2(QbI_E^2 - P) - \frac{1}{2}a\omega P(1 - \frac{3}{2}\omega^2 Lc) \right] = 0
\end{aligned}$$

$$\begin{aligned}
J & \triangleq 1 + \frac{15}{2}bI_E^2 + \frac{81}{4}b^2I_E^4 + \frac{189}{8}b^3I_E^6 + \frac{2835}{256}b^4I_E^8 + \frac{729}{512}b^5I_E^{10} \\
K & \triangleq 1 + 6bI_E^2 + \frac{189}{16}b^2I_E^4 + \frac{135}{16}b^3I_E^6 + \frac{405}{256}b^4I_E^8 \\
P & \triangleq 6 + 36bI_E^2 + \frac{567}{8}b^2I_E^4 + \frac{405}{8}b^3I_E^6 + \frac{1215}{128}b^4I_E^8 \\
Q & \triangleq (2 + 3bI_E^2)(\frac{9}{2} + \frac{27}{2}bI_E^2 + \frac{81}{16}b^2I_E^4)
\end{aligned}$$

Eqs. (6) and (7) are to be solved (for a given V_m) simultaneously for θ and I_E . These equations contain polynomials of degree eleven in I_E , and sine and cosine terms in θ . There are eleven solutions for I_E . Among these solutions, only the positive real ones are acceptable; complex solutions are meaningless and for every negative one there will be a positive solution with a θ of 180° shifted. The number of positive solutions, for a given V_m , indicates the number of 60 Hz steady state modes of operation for the power conditioning system.

We have shown in [9] that for a given input voltage, there is only one acceptable solution of $i_E(t)$ corresponding to a value of choke inductance. That is, if there were no harmonic components in the line and exciting currents, the problem of ferroresonant jump would not exist.

One way to eliminate the multimodal characteristic of the PCS is suggested by the above analysis. It was shown that in the equivalent circuit of Fig. 5, for a given input voltage, there will be only one steady state solution for the exciting current. This implies that by preventing other than 60 Hz currents from flowing into the windings of the saturating transformers, the power conditioning system will always be forced into the desired steady state, regardless of the prior transients. However, it is not practical to have only 60 Hz currents flowing in the windings of the transformers. On the other hand, not all harmonics contribute to the jump problem. To determine which harmonics cause the PCS to become a multistable system, harmonic components must be included in our analysis. Such an analysis, however, is a formidable task.

It is difficult to mathematically identify the harmonic components which contribute to the jump (oscillation) problem and, more importantly, harmonic components found analytically to cause oscillation may not be generated as the result of PCS operation in its environment. Therefore, we will use the actual oscillation data to identify such components. That is, for a PCS installed in its environment, we create a transient which would lead the system to an oscillatory mode of operation. Then, we sample and collect the steady state line currents in time domain. The spectral densities of these time-domain signals are then calculated and analyzed to identify the major harmonics.

For the power conditioning system installed in our laboratory, the necessary transient was created by adding a three-phase wye-connected capacitor bank at its input and energizing it under no load, as shown in Fig. 6. The line currents i_A and i_B were sampled and collected. The current i_A is shown in Fig. 7, its spectral density is plotted in Fig. 8 and tabulated in Table 1.

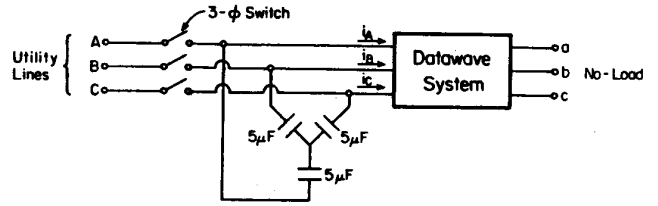


Fig. 6: Creating the transient leading to an oscillatory mode of operation.

It can be seen that the strongest component of the line current has a frequency of about 100 Hz. It is therefore reasonable to, first, suspect this component to be the cause of oscillation; the second candidate would of course be the 15 Hz component.

As a first attempt to force the system into the normal (desired) steady state mode of operation, the 100 Hz component must be suppressed. This can be done by providing low impedance paths to short out the "source" of this harmonic. A delta-connected impedance with the characteristic shown in Fig. 9 will serve our purpose. One way to realize such an impedance characteristic is to use a series LC filter.

The plot of the line current i_A collected during the oscillation test with the new LC filter connected in parallel with the secondary capacitor bank is shown in Fig. 10. Its spectral density is plotted in Fig. 11 and tabulated in Table 2. It can be seen that the system has reached its normal steady state mode of operation. That is, in this case, the choke current is mainly 60 Hz and its no-load magnitude is small as expected.

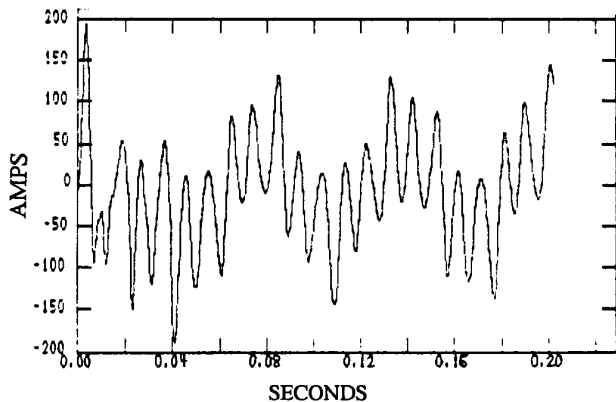


Fig. 7: Choke current — oscillatory operation.

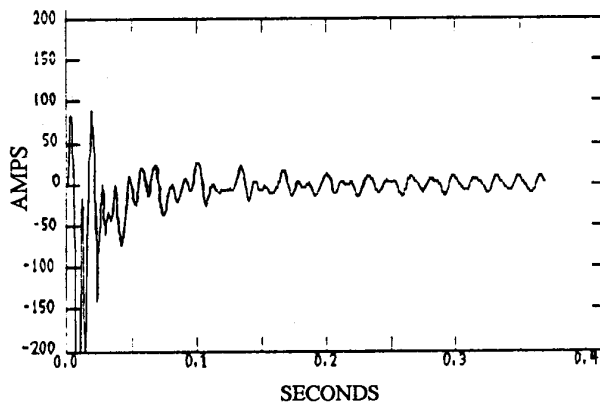


Fig. 10: Choke current — normal operation.

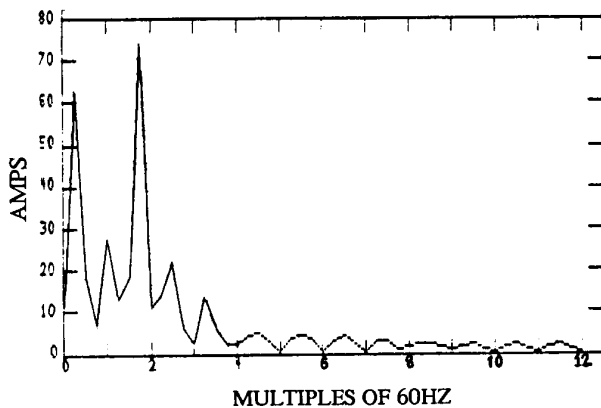


Fig. 8: Choke current spectral density — oscillatory operation.

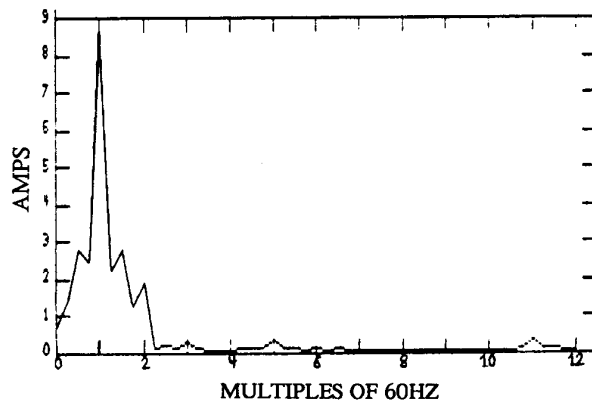


Fig. 11: Choke current spectral density — normal operation.

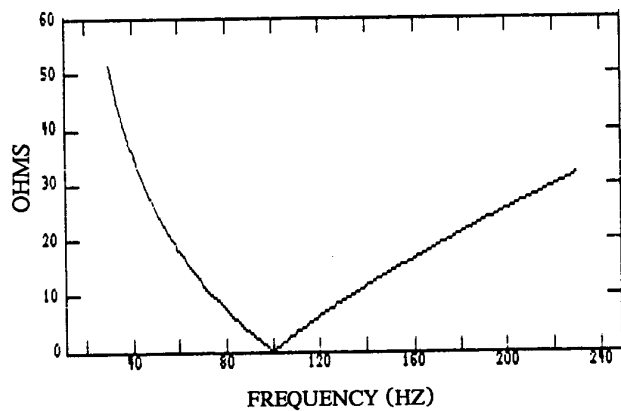


Fig 9: Impedance characteristic for suppression of the 100 Hz component.

Table 1
Fig. 8 in Tabular Form

Freq (Hz)	Amplitude (Amps)	Freq (Hz)	Amplitude (Amps)
0	11.4	90	18.5
15	63.2	105	74.3
30	18.1	120	11.0
45	6.6	135	14.5
60	27.5	150	22.3
75	12.7	180	2.0

Table 2
Fig. 11 in Tabular Form

Freq (Hz)	Amplitude (Amps)	Freq (Hz)	Amplitude (Amps)
0	0.75	90	2.8
15	1.34	105	1.2
30	2.8	120	1.9
45	2.4	135	0.15
60	8.9	150	0.17
75	2.2	180	0.28

Conclusions

The solution to the ferroresonant jump problem was found through the analysis of the power conditioning system steady state behavior. This analysis showed that proper control of the harmonics present in an oscillatory mode can lead to the suppression of the oscillation, and hence, force the system into the desired mode of operation.

The theoretical solution was successfully tested on the power conditioning system installed in our laboratory. That is, an oscillation-causing transient was created through a test. With the system in oscillatory mode, the time-domain samples of one of the input currents were collected and its spectral density was calculated. It was found that the dominating component had a frequency of 100 Hz. Then, a 100 Hz trap was designed and incorporated in the system. Under the same test conditions, no oscillation occurred and the system was forced into the normal mode of operation.

Acknowledgements

The authors wish to thank the Liebert Corporation (a subsidiary of Emerson Electric) for its continuous support of this work. The financial support of the National Science Foundation under Grant ECS-8303330 is acknowledged.

References

- [1] Jeffrey M. Powell, "Polyphase Ferroresonant Voltage Stabilizer Having Input Chokes with Non-Linear Impedance Characteristic," United States Patent 4,305,033, Dec. 8, 1981.
- [2] E.W. Courville, E.M. Gulachenski, and A.O. Kesterson, "A New Device for Improving the Quality of Distribution Feeder Power to Digital Computer and other Voltage-Sensitive Loads," IEEE Trans. PAS, Vol. PAS-101, No. 8, pp. 2916-2924, Aug. 1982.
- [3] G. Sacerdote and D. Pollara, "Saturated Core Type Voltage Stabilizers," Engineering Digest, pp. 547-551, Dec. 1947.
- [4] R.N. Basu, "A New Approach in the Analysis of a Ferroresonant Transformer," IEEE Trans. Mag., Vol. MAG-3, pp. 43-49, March 1967.
- [5] H.P. Hart and R.J. Kakalec, "The Derivation and Application of Design Equations for Ferroresonant Voltage Regulators and Regulated Rectifiers," IEEE Trans. Mag., Vol. MAG-7, No. 1, pp. 205-211, March 1971.
- [6] R. Rudenberg, "Nonharmonic Oscillations as Caused by Magnetic Saturation," Trans. A.I.E.E., Vol. 68I, pp. 676-685, 1949.
- [7] G.W. Swift, "An Analytic Approach to Ferroresonance," IEEE Trans. PAS-88, pp. 42-46, 1969.
- [8] M.S. Maklad and A.A. Zaky, "Multimodal Operation of a Ferroresonant Circuit with Quintic Nonlinearity," IEEE Trans. Mag., Vol. MAG-12, No. 4, pp. 380-384, July 1976.
- [9] S.M. Miri and A. Keyhani, "Models for the Study of Transient and Steady State Behavior of a Three-Phase Power Conditioning System and Improving its Stability Through Analysis, Simulation, and Laboratory Tests," Technical Report, The Ohio State University, Department of Electrical Engineering, June 1987.